2015 Symposium: 13th Imaging Network Ontario Symposium
ImNO Abstract Guidelines (as at Feb 5)

Deadline for Submissions: FEBRUARY 13, 2015

Click HERE to submit your abstract

Before submitting an abstract, we ask that you read the following guidelines carefully. Then, use the online abstract submission form to submit your abstract for consideration at the 13th ImNO Symposium.

The Organizing Committee encourages abstract submissions related to the following consortia:
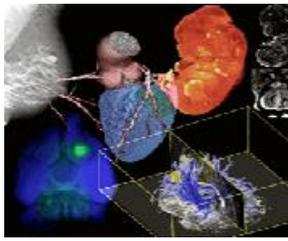
Canadian Atherosclerosis Imaging Network; Medical Imaging Trial Network of Canada
Cancer Imaging Network of Ontario
Ontario Consortium in Imaging for Cardiovascular Therapeutics
OICR Imaging Translation Program
OICR Smarter Imaging Program
Ontario Pre-Clinical Imaging Consortium
Effective Systems for Procedure Specific Healthcare Simulation

When submitting an abstract you will be asked to select a theme from the following list:

Perfusion, Metabolic and Hypoxia Imaging
Small Animal Imaging
Quantitative Imaging
Targeted Probe Development
Imaging Biomarkers
Imaging/Simulation for Therapy Planning
Image Monitoring of Treatment Response
Image Guided Intervention
Visualization and Image Analysis
Instrumentation/Devices

Mandatory Formatting Instructions
- PDF, one (1) page maximum
- Half inch margins on all sides
- Times New Roman 12-point font size
- Abstracts should follow the format: Introduction, Methods, Results, Conclusions
- Any figures and/or images must be embedded on the page
- Title section to include title, authors (indicating primary author), consortium affiliation, institutional affiliations of all authors, and research supervisor (for trainees)
- A sample abstract for formatting reference purposes only may be found below.

Abstract Review Process
The abstracts will be reviewed by the ImNO Scientific Committee. Notifications will be sent to all presenters by February 27, 2015 identifying whether the abstract can be presented as a poster or as an oral presentation, or both. All posters presented by students and trainees at the Symposium will again be reviewed for scientific merit and organization. The top posters from each consortium will be awarded prizes in the poster competition. A small monetary award will also be given. Trainees will be notified about their awards by email within 3 weeks after the Symposium.

Please note: Submission of the abstract constitutes permission for the conference organizers to publish the abstracts in either printed or electronic format
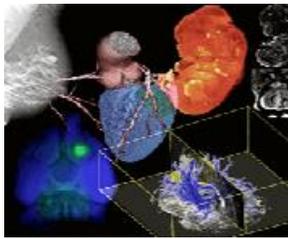

Submission inquiries:
Heather Timm
S•M+i
Strategic Meetings + Incentives
heather.timm@visiontravel.ca

Whole-brain and local receive arrays for imaging non-human primates

Kyle M Gilbert[*], Matthew R DiPrimio, Sarah Hughes, Kathryn Y Manning, and Ravi S Menon
Building a Better Brain: An Ontario Neuroimaging Consortium
Robarts Research Institute, The University of Western Ontario, London, Ontario, Canada

Introduction. High-resolution imaging of the cortex in non-human primates (NHP) is limited by the available SNR. To attain high SNR, receive coils must be in close proximity to the brain. In NHP imaging, this is difficult to achieve due to head fixation posts, chambers, and other external hardware attached to the skull. Implanted coil arrays can avoid this problem and significantly increase SNR in NHP imaging (1). A less invasive approach is to create a tight-fitting coil array that can accommodate the external hardware. The purpose of this study was to design a tight-fitting multi-channel receive coil with whole-brain coverage. A secondary, 7-channel receive coil would then be placed inside a recording chamber (used for electrophysiological measurements) to greatly increase SNR over a 5-mm depth in the peripheral visual cortex (see figure 1). The whole-brain receive coil could then be used as an anatomical reference for the location of the smaller chamber coil. The aim is to significantly increase SNR in V1 to be able to discriminate cortical layers (2).

Methods. A 3D anatomical scan was acquired of a cynomolgus monkey. The images were then converted to a 3D former in CAD, that could be fabricated using rapid-prototype technology. A 16-channel receive array was wound on top of the former; individual loops were sized and located to conform to the brain on the bottom (the posterior – head fixation during scanning) and recording chamber could pass through the two different coil elements). The array was then removed from the former, leaving a sparse wire mesh. Coil elements ranged in diameter from 4 – 5 cm. Loops were constructed from 16-gauge copper wire, with one surface-mount and one variable capacitor for tuning. The coils were connected to low-input-impedance preamplifiers using $n!/2$ cables (~99 cm long; ±5°). Coil matching, active detuning, and preamplifier decoupling were performed on the matching board. A 7-channel array, with 6.2-mm-diameter coils, was mounted on the bottom of a 17-mm-diameter Teflon cylinder that could be inserted into the recording chamber of the monkey. Grooves were machined into the Teflon to allow coils to be optimally overlapped and to lay flat on the bottom of the cylinder. Twisted pairs of wire were routed through the cylinder to a tuning capacitor and lattice balun mounted on the opposite end of the cylinder. Lattice baluns were connected to preamplifiers with $n!/2$ cables. No discrete components were located on the coil elements. The transmit coil consisted of two rectangular loops (16.5 ″ 15.2 cm) that were capacitively decoupled. The transmit coil could be placed above the head of the monkey to increase transmit efficiency, or below the head to increase access (at the expense of transmit efficiency).

All performance measurements were acquired on a 7-T human MRI system with a head gradient insert. Signal measurements were recorded using 2D FLASH sequences with both receive coils active. The coils were loaded with a 6.4-cm-diameter phantom filled with 80-mM NaCl and 20-mM $CuSO_4$. Noise correlation was calculated from a noise-only scan with a 1-MHz bandwidth. Whole-brain images were acquired with the 16-channel whole-brain coil while the monkey was positioned headfirst in the sphinx position (TE/TR: 8/1100 ms, matrix: 256 ″ 256, FOV: 9.6 ″ 9.6 cm, thickness: 1 mm, N_{slices}: 36, bw: 31 kHz, flip angle: 45°).

Results. The noise correlation of the two coils is shown in figure 2; the noise between the two coil arrays is highly independent. Elements on the whole-brain coil array achieved a minimum and mean S_{12} of -17 dB and -22 dB, respectively. Preamplifier decoupling increased isolation by 15 dB, and active detuning provided an additional 6 dB during transmission. The chamber coil array achieved S_{12} values of better than -22 dB, and a 28-dB isolation to the nearest coil element on the whole-brain receive array. Despite the small coil size, preamplifier decoupling was capable of increasing the mean isolation by 13 dB, and active detuning provided an additional 6 dB isolation during transmission.

The 3 – 8 fold increase in signal was produced by the chamber coil array, over a 5-mm depth in the periphery of the phantom, compared to the whole-brain coil array (figure 3). An anatomical image of an NHP is shown in figure 4. Images show excellent coverage in the visual cortex, despite coils in close proximity to the visual cortex being partially orthogonal to the static field. The coil is able to see the entire brain with uniform contrast.

Conclusions. The utility of employing two separate receive arrays to provide whole-brain coverage of NHPs, while simultaneously significantly increasing SNR in a localized region, is shown. Both coil arrays have the ability to accelerate, creating the potential for high-resolution anatomical and functional imaging.

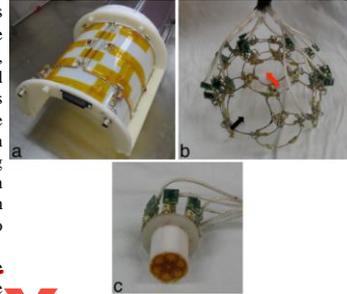**References.** [1] Janssens *et al.* Neuroimage 2012;62:1529-1536. [2] Chen *et al.* Neuroimage 2012;59:3441-3449.

Figure 1. A photograph of **(a)** the transmit coil, **(b)** whole-brain coil, and **(c)** chamber coil. Feed-through locations of the head post and chamber are provided by the red and black arrows, respectively.
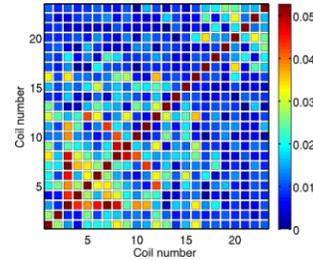

Figure 2. S_{12} matrix for the whole-brain coil (ch. 1-16) and chamber coil (ch. 17-23).
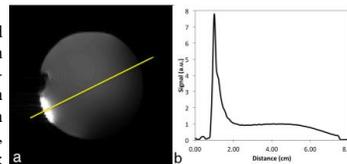

Figure 3. (a) An image acquired with both the 16-channel whole-brain coil and 7-channel chamber coil active. **(b)** The resultant signal profile.
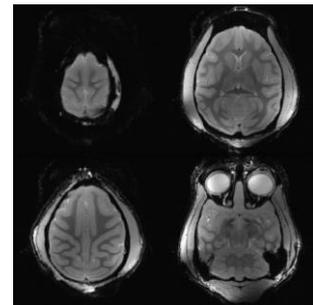

Figure 4. Four slices of an image acquired with the 16-channel whole-brain coil.